CHEMISTRY
A EUROPEAN JOURNAL

DOI: 10.1002/chem.201000040

Self-Assembly, Disassembly, and Reassembly of Gold Nanorods Mediated by Bis(terpyridine)–Metal Connectivity

Yi-Tsu Chan,[a] Sinan Li,[b] Charles N. Moorefield,[c] Pingshan Wang,[d] Carol D. Shreiner,[e] and George R. Newkome*[a]

Since the advent of nanotechnology, a primary challenge has been to assemble materials from predesigned building blocks for the fabrication of nanometer-sized materials. Metal nanocrystals (NCs) have attracted significant attention due to their unique shape and size, as well as their tuneable electrical, optical and catalytic properties.[1] A bottom-up approach has generally been used for constructing the desired multi-unit composites from individual components. Although extensive studies have been performed on spherically shaped NCs, research on anisotropic nanoparticles, for example, nanorods (NRs)[2] with a distinct 1D or linear structure, is limited. Since the properties of NCs are mostly size- and shape-dependent, NRs have the potential to show novel as well as improved properties, such as in surface-enhanced Raman scattering (SERS) effects or optical and fluorescent properties,[2a] when compared to isotropic nanospheres (NSs).[1b,c,3] Geometrically, the aspect ratio (the length of major axis divided by the width of minor axis) of NRs is >1 and their cofacial assembly produces more angularly complex structures than that of the NSs.[4] Side-to-side assemblies of NRs have been achieved by introducing active sites on the sides of the rods and subsequently connecting via DNA, electrostatic interaction,[5] and more recently with click chemistry;[6] however, arrangement of NRs in an end-to-end orientation, for example, forming chains or branched structures, requires a regiospecific functionalization. Toward this goal, the tips of NRs have been modified with different metals, which were subsequently termed nanodumbbells, for participation in direct end-to-end assembly.[7]

It is well-known that Au NRs have different crystallographic facets, which comprise the ends and side surfaces.[8] Recently, it was found that these side facets have a higher surface energy, and in turn, adsorb more bilayer surfactant, for example, cetyltrimethylammonium bromide (CTAB);[9] notably, the yield of these surface-modified nanorods has been shown to be supplier (CTAB) dependent.[10] Current progress on direct end-to-end Au NR assembly has focused on using biocompatible connectors,[11] α,ω-dithiols,[12] and synthetic polymers.[13] As well, organometallic connections, such as bis(terpyridine)-transition metal complexes, are also of interest due to their potential to impart unique electrical, optical, and photovoltaic properties.[14] For example, hybrid Au NCs and bis(terpyridine)–Ru^{II} complexes have been fabricated and shown to exhibit enhanced electrochemical properties.[15] Herein, we report the first example of a bottom-up approach for the end-to-end linear and branched assembly of Au NRs into multicomponent structures using [(disulfide-modified terpyridine)$_2$–M^{II}] (M = Fe or Cd) interconnectors and their facile disassembly and reassembly.

The synthesis of disulfide-modified monoterpyridine (SS-tpy) **2**, the [(SS-tpy)$_2$–M^{II}] complexes **3** (M = Fe), and **4** (M = Cd) is shown in Scheme 1. In a typical Gabriel synthesis, 4′-(4-hydroxyphenyl)-2,2′:6′2″-terpyridine[16] was treated with *N*-(3-bromopropyl)phthalimide to afford the intermediate protected amine, which was subsequently deprotected ($H_2NNH_2{\cdot}H_2O$) to give the amine-modified monoterpyridine **1**. The structure was supported (^{1}H NMR) by signals for the new OCH_2 (4.17 ppm) and CH_2NH_2 (3.20 ppm) moieties; a dominate peak (ESI-MS) at m/z 383.3 $[M+H]^+$ further confirms the structure. Disulfide-modified monoterpyridine **2**

[a] Y.-T. Chan, Prof. Dr. G. R. Newkome
Departments of Polymer Science and Chemistry
The University of Akron, Akron, OH 44325-4717 (USA)
Fax: (+1) 330-972-2413
E-mail: newkome@uakron.edu

[b] Dr. S. Li
Excel Polymers, 14330 Kinsman Rd.
Burton, OH 44325 (USA)

[c] Dr. C. N. Moorefield
Maurice Morton Institute for Polymer Science
The University of Akron, Akron, OH 44325 (USA)

[d] Dr. P. Wang
ChemNano Materials, 2220 High St. Suite 605
Cuyahoga Falls, OH 44221 (USA)

[e] Prof. Dr. C. D. Shreiner
Chemistry Department, Hiram College, P.O. Box 67
Hiram, OH 44234 (USA)

Supporting information for this article is available on the WWW under http://dx.doi.org/10.1002/chem.201000040.

was prepared via diimide-mediated amidation of monoterpyridine **1** using thioctic acid (TA). The transformation was indicated by the appearance of a new signal (^{13}C NMR) at 173.0 ppm attributed to the amide carbonyl carbon; peaks (ESI-MS) at *m*/*z* 571.4 amu $[M+H]^+$ and 593.3 amu $[M+Na]^+$ provided further confirmation. Reaction of terpyridine **2** with 0.5 equiv of either $FeCl_2\cdot 4H_2O$ or $Cd(NO_3)_2\cdot 4H_2O$ gave rise to the $[(SS\text{-}tpy)_2\text{–}M^{II}]$ connective linkers **3** (M = Fe) and **4** (M = Cd), respectively. Their ^{1}H NMR, ^{13}C NMR, and ESI-MS spectra agreed with the structures given in Scheme 1 (see the Supporting Information).

The seed-mediated growth method[17] was applied to synthesize the Au NRs, whereby spherical Au NPs were produced as seeds by chemical reduction of $HAuCl_4\cdot 3H_2O$, followed by the addition of a surfactant (CTAB) template. The Au NRs were purified by centrifuging the mixture at 7000 rpm for 10 min and possessed an average aspect ratio of about 4.2, as determined by TEM imaging (Figure 1 A). UV/Vis spectroscopy was used to characterize the two absorption bands of the Au NRs, which consisted of the transverse and longitudinal plasmon bands (512 and 716 nm, respectively) (Figure 3 A). In distilled water, the Au NRs are stable for months.

NR connectivity (Scheme 2) was effected by adding 100 μL of a stock solution [27 μM in MeOH/MeCN/H_2O 1:1:1 *v*/*v*/*v*] of the iron-complexed connector **3** to 1 mL of Au NR aqueous solution, sonicated for 10 min, and left undisturbed at 25 °C for two days to afford a purple $<(Au\ NR)[(SS\text{-}tpy)_2\text{-}Fe^{II}]_n>_m$ precipitate that was collected by centrifuging (3000 rpm, 5 min) and removal of the supernatant.

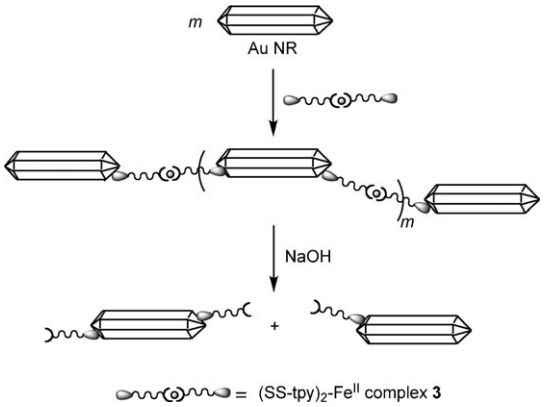

Scheme 2. Idealized $<(Au\ NR)[(SS\text{-}tpy)_2\text{-}Fe^{II}]_n>_m$ formation.

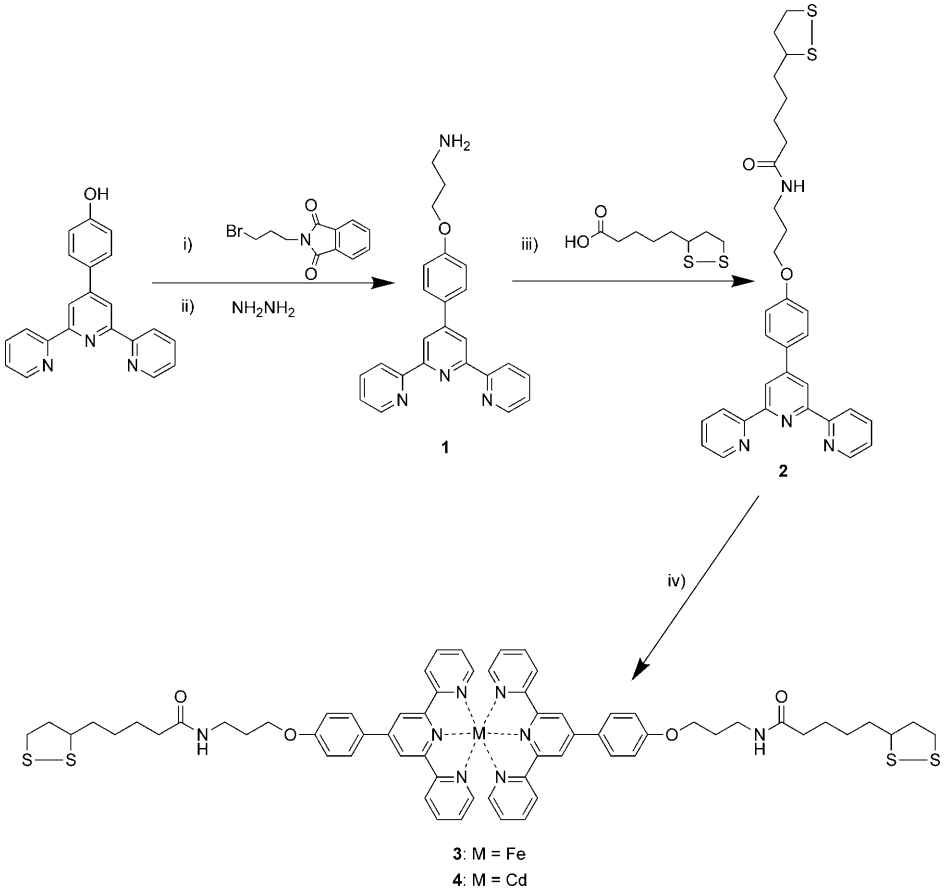

Scheme 1. Synthesis of complexes **3** and **4**: i) K_2CO_3, MeCN, reflux, N_2, 10 h; ii) EtOH, reflux, 4 h; iii) DCC, HOBT, CH_2Cl_2, 25 °C, 18 h; iv) $FeCl_2\cdot 4H_2O$ for **3** and $Cd(NO_3)_2\cdot 4H_2O$ for **4**, respectively (each dimer isolated as the PF_6^- salt; see the Supporting Information).

X-ray photoelectron spectroscopy (XPS, monochromatic $Mg_{K\alpha}$ radiation, 250 W, 93.90 eV) of the Au NRs (Figure S1A) revealed typical gold peaks at Au 4f7 (84.0 eV) and Au 4f5 (87.7 eV), which were also used as reference peaks. Bromine peaks (3p3 at 180.4 eV and 3p1 at 187.0 eV), generated exclusively from CTAB, were also detected. Since the $<(Au\ NR)[(SS\text{-}tpy)_2\text{-}Fe^{II}]_n>_m$ hybrid only possesses small portions of the $[(SS\text{-}tpy)_2\text{-}Fe^{II}]$ connectors, the XPS spectrum exhibited the appearance of new peaks at 708.7 and 721.4 eV, which were attributed to Fe 2p3 and Fe 2p1, respectively (Figure S1B), as well as new S 2p peaks (163.7 and 168.9 eV).

TEM was used to image the structures and shapes of the uncomplexed Au NRs and their subsequent assemblies. It is well-known that Au NRs can appear to be physically bound with no added connecting agent[1d] under TEM imaging:

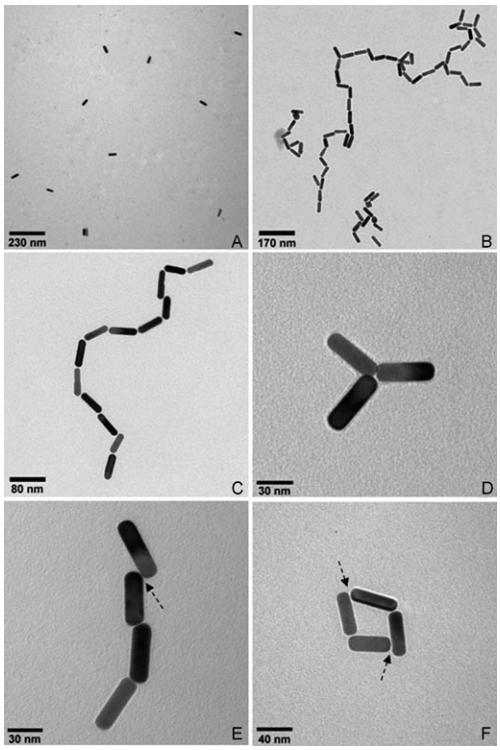

Figure 1. Representative TEM images for the native, untreated Au NRs (A), and $<$(Au NR)[(SS-tpy)$_2$-Fe^{II}]$_n>_m$ hybrids (B–F): B) in low magnification; C) linear end-to-end connectivity; D) a branched structure; E) end-to-end as well as end-to-wall connectivity; F) a cyclic structure.

in our case, $>95\%$ of the freshly prepared Au NRs were found to be monomeric and $<5\%$ were dimers (i.e., Au NR-Au NR). After assembly using the [(SS-tpy)$_2$-Fe^{II}] complex, few individual Au NRs were detected in the TEM (Figure 1B). Since the side faces of the Au NRs are densely protected with a CTAB bilayer, the disulfide groups of the [(SS-tpy)$_2$-Fe^{II}] connector preferentially, but not exclusively, attack the tips of the Au NRs, leading to predominately end-to-end assemblies. A linear polymeric (Figure 1C) structure of the hybrid was clearly observed in the TEM images. Branched structures were also observed (Figure 1D) and attributed to multiple functionalities distributed on the tips of the rods. Although end-to-end assembly predominates, some connections showed end-to-wall (arrows in Figure 1E and F) attachment, which can be attributed to side-wall CTAB displacements by connectors. The average distance (Figure 2) between gold nanorods is less than 3 nm which is consistent with the calculated molecular length of the [(SS-tpy)$_2$-Fe^{II}] complex (complete extended length: 4.6 nm and central rigid section length: 2 nm).

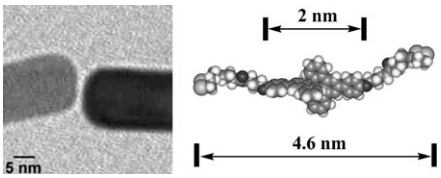

Figure 2. A high magnification TEM image of end-to-end NR connectivity showing a separation that corresponds well with the calculated length of the extended, space-filling representation of the [(SS-tpy)$_2$-Fe^{II}] complex.

Further confirming the assembly of the $<$(Au NR)[(SS-tpy)$_2$-Fe^{II}]$_n>_m$ hybrids, UV/Vis absorption data for the transverse plasmon bands at ~512 nm in Figure 3A and B showed no significant difference. However, a new absorption band at 572 nm was observed and assigned as the metal–ligand charge-transfer (MLCT) transition,[14a] which was attributed to the promotion of an electron from the Fe^{II}-centered d orbitals to unfilled ligand π^* orbitals of the [(SS-tpy)$_2$-Fe^{II}] complex (the MLCT band for individual [(SS-tpy)$_2$-Fe^{II}] in MeOH at $\lambda_{max}=573$ nm). An intense ligand-centered π–π^* transition of the terpyridine components in the [(SS-tpy)$_2$-Fe^{II}] can be clearly seen as the absorption peaks at $\lambda_{max}=286$ and 323 nm. Furthermore, the longitudinal plasmon band shows a red-shift (from 716 to 770 nm) and a broadened shape, accompanied by a decrease in the absorption intensity. This spectral change is interpreted as the interplasmon coupling of Au NR assembly in the longitudinal direction and indicates an orientation of the Au NRs into linear chains via the end-to-end connectivity.[11c,d]

Since [(tpy)$_2$-Fe^{II}]-based complexes have been demonstrated[18] to be unstable under basic conditions, an NaOH solution (1 mM) was added to the hybrid causing a rapid disassembly to generate individual Au NRs (Figure S2A). The disassembled Au NRs were collected by centrifuging at 7000 rpm for 10 min, followed by removal of the supernate and then redispersed into 1 mL distilled water. The XPS

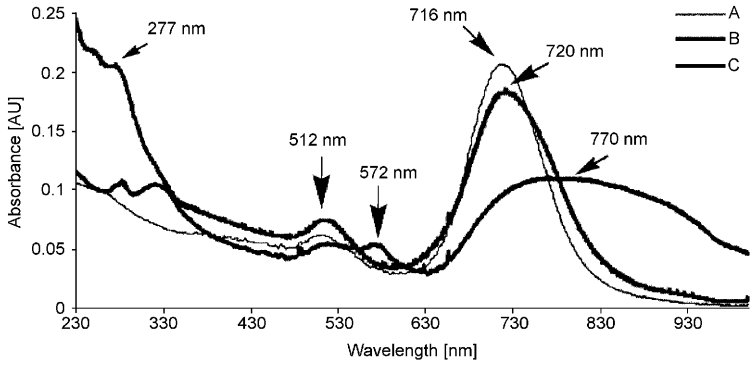

Figure 3. UV/Vis spectra of A) Au NRs, B) $<$(Au NR)[(SS-tpy)$_2$-Fe^{II}]$_n>_m$ hybrids, and C) disassembled SS-tpy-modified Au NRs.

spectrum (Figure S1C) showed small portions of S 2p peak, and the total disappearance of Fe peaks, which proves that the disassembled Au NRs possess the metal (iron)-free, tpy-modified end-groups. Comparison of the UV spectrum of the free Au NRs (Figure 3A) and the Au NR hybrids (Figure 3B), the disassembled material (Figure 3C) showed the disappearance of the MLCT band at $\lambda_{max}=572$ nm for the [(SS-tpy)$_2$-Fe^{II}] connectivity; whereas, the absorption bands at $\lambda_{max}=254$ and 277 nm for the free SS-tpy moieties were still present. This facile disassembly showed the reversibility of the $<$(Au NR)[(SS-tpy)$_2$-Fe^{II}]$_n>_m$ composite and the retention of the free terpyridine ligands on the surface of the gold nanorods. In order to reconnect these terpyridine-modified gold nanorods, a $FeCl_2$ solution (100 μL, 27 μM in H_2O) was added into the disassembled Au NRs. After sonication for 10 min, transverse and longitudinal plasmon UV/Vis bands showed no obvious difference (Figure S3) and only individual nanorods were observed in the TEM images (Figure S2B); however, a band at 572 nm was again observed in UV/Vis. These results suggest a facile intramolecular complexation[19] of Fe^{II} ions between two terpyridines on the same nanorod tip (Scheme 3A; notably, the number of end-bound terpyridines varies) enhanced by a rapid complexation rate[20] and a longer incubation period for nanochain formation.[11c]

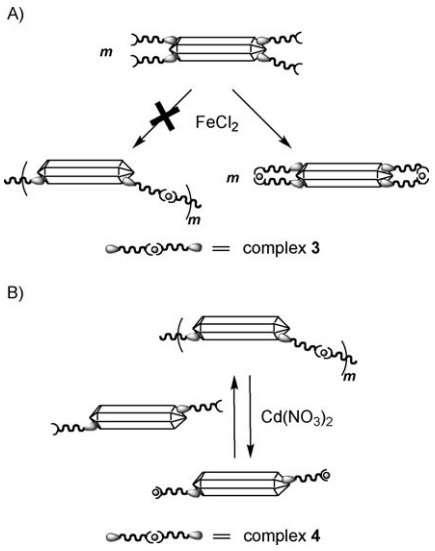

Scheme 3. Idealized representations of intramolecular vs. intermolecular complexations: A) Complexation reaction of terpyridine-modified Au NRs and $FeCl_2$; B) disassembled and reassembled reactions of terpyridine-modified Au NRs.

Attempts to verify the Fe^{II}-based connectivity of the hybrids by disassembly and reassembly were unsuccessful due to the strong Fe^{II}–terpyridine coordination ($K_1=1.3\times10^7\,M^{-1}$)[14a] that is not easily dissociated without harsh conditions or an added strong nucleophile (i.e., HO^-). Investigations using Cd^{II}, a weaker coordinating species ($K_1=1.3\times10^5\,M^{-1}$),[14a] were subsequently undertaken. Thus, the $<$(Au NR)[(SS-tpy)$_2$-Cd^{II}]$_n>_m$ hybrid was obtained using the labile linker complex **4**. Reversibility of the tpy–Cd^{II}–tpy linker **4** was subsequently demonstrated by adjusting the ligand-to-metal ratio. Treatment of terpyridine **2** with 0.5 equiv of $Cd(NO_3)_2\cdot4H_2O$ gave rise to **4** with intermolecular connectivity, which exhibited an upfield shift (^{1}H NMR; Figure 4B) from 8.74 to 8.07 ppm of the doublet assigned to the 6,6″-tpy*H*s due to the octahedral geometry. Upon addition of another 0.5 equiv of $Cd(NO_3)_2\cdot4H_2O$, the bis(terpyridine) complex **4** dissociated into the SS-monotpy–Cd^{II} adducts that were verified by a comparable downfield shift of the 6,6″-tpy*H*s from 8.07 to 8.87 ppm (Figure 4C). Moreover, the mono-terpyridine–Cd$(H_2O)(NO_3)_2$ adduct has been reported in the presence of excess $Cd(NO_3)_2\cdot4H_2O$.[21] Reassembly of the hybrid with added additional Cd^{II} was not feasible; however, since Cd^{II}-based complexes are demonstrably more labile than the corresponding Fe^{II}-based complexes, the (Au NR)-(SS-monotpy-Cd^{II})$_n$ hybrids (Scheme 3B) were obtained by disassembling the $<$(Au NR)-[(SS-tpy)$_2$-Cd^{II}]$_n>_m$ chain with an excess of $Cd(NO_3)_2\cdot4H_2O$ (unreacted Cd^{II} was removed by centrifugation), and used to inhibit the intramolecular complexation on the surface of Au NRs. Reassembly was achieved by mixing the free terpyridine-modified (donor) Au NRs and the tpy-Cd^{II}-modified (acceptor) Au NRs. A red-shift (from 717 to 783 nm) was again observed in the UV/Vis spectrum of the reassembled Au NRs (Figure S4).

We have synthesized [(disulfide-terminated tpy)$_2$-M^{II}] complexes and employed them in the predominately end-to-end assembly of Au NRs; facile disassembly occurred upon treatment with aqueous NaOH solution for the Fe^{II} linker

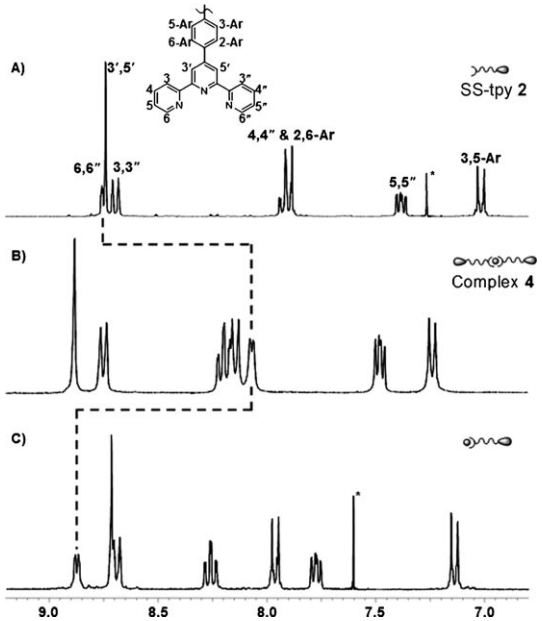

Figure 4. Aromatic region of ^{1}H NMR spectra for the A) SS-tpy **2** in $CDCl_3$, B) bis(terpyridine) complex **4** in CD_3CN, and C) SS-monotpy–Cd^{II} adduct in $CDCl_3/CD_3OD$ 1:1. The marked peak * corresponds to $CHCl_3$.

and excess $Cd(NO_3)_2 \cdot 4H_2O$ for the Cd^{II} linker, respectively. XPS, UV/Vis, and TEM experiments were used to confirm the predominately end-to-end assembly, as well as structural disassembly. Attempted inter-NR reassembly of the tpy-Fe-tpy connector was not realized but rather intra-NR complexation occurred. The reassembly was achieved by mixing the donor-modified and the acceptor-modified Au NRs. This simple method can be used to construct more complicated multicomponent nanoarchitectures and it gives rise to the incorporation of organometallic species that facilitates access to their unique properties.

Acknowledgements

We thank the National Science Foundation for generous financial support (DMR-0705015).

Keywords: cadmium · iron · nanoparticles · self-assembly · tridentate ligands

[1] a) R. Shenhar, V. M. Rotello, *Acc. Chem. Res.* **2003**, *36*, 549–561; b) M. A. El-Sayed, *Acc. Chem. Res.* **2001**, *34*, 257–264; c) K. G. Thomas, P. V. Kamat, *Acc. Chem. Res.* **2003**, *36*, 888–898; d) J. Perez-Juste, I. Pastoriza-Santos, L. M. Liz-Marzan, P. Mulvaney, *Coord. Chem. Rev.* **2005**, *249*, 1870–1901.

[2] a) C. J. Murphy, T. K. Sau, A. M. Gole, C. J. Orendorff, J. Gao, L. Gou, S. E. Hunyadi, T. Li, *J. Phys. Chem. B* **2005**, *109*, 13857–13870; b) C. J. Murphy, A. M. Gole, S. E. Hunyadi, C. J. Orendorff, *Inorg. Chem.* **2006**, *45*, 7544–7554.

[3] S. K. Ghosh, T. Pal, *Chem. Rev.* **2007**, *107*, 4797–4862.

[4] C. J. Murphy, N. R. Jana, *Adv. Mater.* **2002**, *14*, 80–82.

[5] a) E. Dujardin, L.-B. Hsin, C. R. C. Wang, S. Mann, *Chem. Commun.* **2001**, 1264–1265; b) A. Gole, C. J. Murphy, *Langmuir* **2005**, *21*, 10756–10762; c) A. Gole, C. J. Orendorff, C. B. Murphy, *Langmuir* **2004**, *20*, 7117–7122; d) C. J. Orendorff, P. L. Hawkins, C. J. Murphy, *Langmuir* **2005**, *21*, 2022–2026.

[6] A. Gole, C. J. Murphy, *Langmuir* **2008**, *24*, 266–272.

[7] a) A. K. Salem, M. Cgen, J. Hayden, K. W. Leong, P. C. Searson, *Nano Lett.* **2004**, *4*, 1163–1165; b) M. Chen, L. Guo, R. Ravi, P. C. Searson, *J. Phys. Chem. B* **2006**, *110*, 211–217; c) A. Salant, E. Amitay-Sadovsky, U. Banin, *J. Am. Chem. Soc.* **2006**, *128*, 10006–10007; d) > Y. Wang, Y. F. Li, Y. Song, C. Z. Huang, *Chem. Commun.* **2010**, 1332–1334.

[8] a) Z. L. Wang, M. B. Mohamed, S. Link, M. A. El-Sayed, *Surf. Sci.* **1999**, *440*, L809 L814; b) Z. L. Wang, R. P. Gao, B. Nikoobakht, M. A. El-Sayed, *J. Phys. Chem. B* **2000**, *104*, 5417–5420.

[9] a) L. Gou, C. J. Murphy, *Chem. Mater.* **2005**, *17*, 3668–3672; b) B. Nikoobakht, M. A. El-Sayed, *Langmuir* **2001**, *17*, 6368–6374.

[10] D. K. Smith, B. A. Korgel, *Langmuir* **2008**, *24*, 644–649.

[11] a) K. K. Caswell, J. N. Wilson, U. H. F. Bunz, C. J. Murphy, *J. Am. Chem. Soc.* **2003**, *125*, 13914–13915; b) J.-Y. Chang, H. Wu, H. Chen, Y.-C. Ling, W. Tan, *Chem. Commun.* **2005**, 1092–1094; c) S. T. S. Joseph, B. I. Ipe, P. Pramod, K. G. Thomas, *J. Phys. Chem. B* **2006**, *110*, 150–157; d) K. G. Thomas, S. Barazzouk, B. I. Ipe, S. T. Joseph, P. V. Kamat, *J. Phys. Chem. B* **2004**, *108*, 13066–13068.

[12] a) P. Pramod, K. G. Thomas, *Adv. Mater.* **2008**, *20*, 4300–4305; b) S. T. S. Joseph, B. I. Ipe, P. Pramod, K. G. Thomas, *J. Phys. Chem. B* **2005**, *109*, 150–157.

[13] a) Z. Nie, D. Fava, E. Kumacheva, S. Zou, G. C. Walker, M. Rubinstein, *Nat. Mater.* **2007**, *6*, 609–614; b) Z. Nie, D. Fava, M. Rubinstein, E. Kumacheva, *J. Am. Chem. Soc.* **2008**, *130*, 3683–3689; c) D. Fava, Z. Nie, M. A. Winnik, E. Kumacheva, *Adv. Mater.* **2008**, *20*, 4318–4322; d) D. Fava, M. A. Winnik, E. Kumacheva, *Chem. Commun.* **2009**, 2571–2573.

[14] a) U. S. Schubert, H. Hofmeier, G. R. Newkome, *Modern Terpyridine Chemistry*, Wiley-VCH, Weinheim, **2006**; b) T. B. Norsten, B. L. Frankamp, V. M. Rotello, *Nano Lett.* **2002**, *2*, 1345–1348; c) R. Shenhar, E. Jeoung, S. Srivastava, T. B. Norsten, V. M. Rotello, *Adv. Mater.* **2005**, *17*, 2206–2210; d) P. Arumugam, D. Patra, B. Samanta, S. S. Agasti, C. Subramani, V. M. Rotello, *J. Am. Chem. Soc.* **2008**, *130*, 10046–10047; e) W. R. McNamara, R. C. Snoeberger, G. Li, J. M. Schleicher, C. W. Cady, M. Poyatos, C. A. Schmuttenmaer, R. H. Crabtree, G. W. Brudvig, V. S. Batista, *J. Am. Chem. Soc.* **2008**, *130*, 14329–14338.

[15] M. Ito, T. Tsukatani, H. Fujihara, *J. Mater. Chem.* **2005**, *15*, 960–964.

[16] Y.-T. Chan, C. N. Moorefield, G. R. Newkome, *Chem. Commun.* **2009**, 6928–6930.

[17] B. Nikoobakht, M. A. El-Sayed, *Chem. Mater.* **2003**, *15*, 1957–1962.

[18] P. Wang, C. N. Moorefield, G. R. Newkome, *Angew. Chem.* **2005**, *117*, 1707–1711; *Angew. Chem. Int. Ed.* **2005**, *44*, 1679–1683.

[19] G. R. Newkome, K. S. Yoo, C. N. Moorefield, *Chem. Commun.* **2002**, 2164–2165.

[20] R. H. Holyer, C. D. Hubbard, S. F. A. Kettle, R. G. Wilkins, *Inorg. Chem.* **1966**, *5*, 622–625.

[21] J. Granifo, M. Garland, R. Baggio, *Inorg. Chem. Commun.* **2004**, *7*, 77–81.

Received: January 8, 2010
Published online: March 16, 2010

